Resonant Pulling of a Microparticle Using a Backward Surface Wave

A. V. Maslov*
University of Nizhny Novgorod, Nizhny Novgorod 603950, Russia
(Received 18 July 2013; published 18 March 2014)

It is predicted that the optical force experienced by a dielectric particle excited resonantly by a surface wave can be directed opposite to the incident power flow when the exciting wave is a backward one. This is consistent with the electromagnetic momentum flow of the backward wave being directed opposite to the power flow. The magnitude of the force can be comparable to the momentum flow of the surface wave. Such forces bring a deeper understanding of the electromagnetics of backward surface waves and can be used in integrated photonic circuits and optofluidic devices.

DOI: 10.1103/PhysRevLett.112.113903 PACS numbers: 42.25.Fx, 42.50.Wk, 42.82.Et

The existence of electromagnetic forces acting on polarizable objects follows from Maxwell's theory [1]. The small value of these forces, however, delayed their experimental confirmation until the measurement of radiation pressure by Lebedev [2]. After the invention of laser, the optical forces enabled the manipulation of micro-objects [3], but their magnitude remained small due to the low refractive index contrast, especially in liquids. The scattering and the forces can be increased by using resonances, for example, whispering gallery modes (WGMs) in dielectric microparticles. It was calculated [4] and measured [5] that the scattering of a plane wave by a microsphere produces resonant peaks of force. Although the peaks were narrow, their magnitude was not very large due to the weak coupling of the WGMs to laser beams. To increase it, the evanescent fields of waveguides or total-internal-reflection prisms can be used.

Multiple applications of WGMs [6] stimulated renewed interest in resonant optical forces. Optofluidic technologies may allow manipulation and sorting of the particles according to their WGM resonances. Although the resonant forces excited by evanescent tails were studied theoretically [7–9], the size deviations in the particle ensemble prevented their registration [7].

Recent experiments demonstrated that microspheres near an optical fiber can experience propelling forces whose magnitudes were estimated to reach an equivalent of ~60% of power absorption, based on Stokes's law [10]. The giant resonant force was interpreted as being due to the excitation of a WGM during which a large portion of the incident electromagnetic momentum flow is converted into the propelling force [11].

The efficient momentum-to-force conversion in the system consisting of a waveguide and a WGM particle opens new research directions. One interesting question is, what happens when the exciting wave is a backward one, i.e., has the phase and group velocities in the opposite directions? Would the optical force be negative so that is to pull the particle towards the source of energy? How is the force related to the electromagnetic momentum flow of the backward wave? How is the momentum flow related to the power flow? These fundamental questions are investigated in this Letter. In particular, it is shown that a backward wave can indeed create a pulling force.

In addition to its fundamental importance, the momentum exchange between a backward wave and a WGM resonator is a new way of creating an optical pulling force, which attracted attention recently due to its peculiar nature and applications for particle manipulation. Initially, the existence of a pulling force created by a Bessel beam was found in acoustics [12,13]. Later, the pulling force under illumination by a Bessel beam was shown to exist in optics [14]. The experimental demonstration of a tractor effect using a solenoid beam, which can be expressed as a superposition of copropagating Bessel beams, was reported in Ref. [15]. The Bessel beams can be replaced by strongly nonparaxial beams [16] or a superposition of plane waves steeply angled towards each other [17,18]. The pulling force can also be generated by bichromatic copropagating beams [19]. The direction of the force can be controlled using two counterpropagating beams [20] or copropagating beams with varying phase between them [21] in the so-called optical conveyor. The pulling force was created by free-space beams in Refs. [12–21].

It was also suggested that a backward wave may create a reverse force on a dipole [22]. The proposed backward-wave structure was either a waveguide with a high permittivity dielectric rod [23] or an array of such rods [22]. However, the properties of the reverse force were not investigated. The appearance of the reverse force was deduced from the formula in which the force is determined only by the incident wave. It neglects the field induced by the dipole itself due to the interaction with the structure.

In this Letter, we address the use of backward surface waves to efficiently excite WGMs in a particle and create forces with magnitudes comparable to the momentum flow of the incident wave. We rigorously account for the strong interaction between the waveguiding structure and the

WGM resonator. The use of backward guided waves can be compatible with modern optofluidic technologies and can also expand the optomechanical properties of various integrated photonic circuits [24–27]

Our physical model consists of a particle with dielectric constant ε_s located at a distance d from a plasma slab; see Fig. 1(a). The plasma slab is chosen based on its ability to support both backward and forward waves [28]. An initial surface wave is scattered by the particle and creates a force. We consider a two-dimensional case (no dependence on z) and assume a $e^{-i\omega t}$ dependence for all complex fields $\{E_x, E_y, H_z\}$.

The initial guided wave with the propagation wave number h_0 has a symmetric profile of H_z:

$$H_z(x,y) = H_0 e^{ih_0 x} \begin{cases} e^{-\varkappa_b(|y|-L/2)} & |y| > L/2 \\ \frac{\cosh(\varkappa_p y)}{\cosh(\varkappa_p L/2)} & |y| < L/2, \end{cases} \quad (1)$$

where $\varkappa_{p,b} = \sqrt{h_0^2 - \varepsilon_{p,b}\omega^2/c^2}$ are the evanescent (transverse) wave numbers in the plasma and background, respectively. The dielectric constant of the plasma slab is $\varepsilon_p(\omega) = 1 - \omega_p^2/\omega^2$, where ω_p is the plasma frequency.

The dispersion properties of mode (1) are shown in Fig. 2. The dispersion curve has intervals that correspond to forward and backward waves. For a given ω, a backward wave and a forward wave coexist but have different wave numbers h. The backward wave has a larger h and, therefore, decays faster outside of the slab. Large values of h are of little interest since the decay rate $\varkappa_b$ becomes very large for the coupling to the particle. It seems practical to work at $hc/\omega \sim 1-2$. In this regime, both waves have comparable values of h and that can lead to the intermode energy conversion due to the scattering.

We choose $L\omega_p/c = 0.2$ and fix the operating frequency on the dispersion curve, see Fig. 2: $h_b c/\omega_p = 1.5$, $h_f c/\omega_p = 1.248$, $\omega/\omega_p = 0.9123$ ($\varepsilon_p = -0.2014$). These values correspond to phase indices $n_b = ch_b/\omega = 1.644$ and $n_f = ch_f/\omega = 1.368$. We will consider two cases, A and B; see Fig. 1(b). In case A, the incident wave is the backward one ($h_0 = h_b$) and originates at $x \to +\infty$. In case B, the incident wave is the forward one ($h_0 = h_f$) and originates at $x \to -\infty$. In both cases, $h_0 > 0$, and the phase of the incident wave moves in the $+x$ direction. We use $\varepsilon_b = 1$ and $\sqrt{\varepsilon_s} = 1.4$. The scattering properties of such a particle in free space are included in Ref. [11].

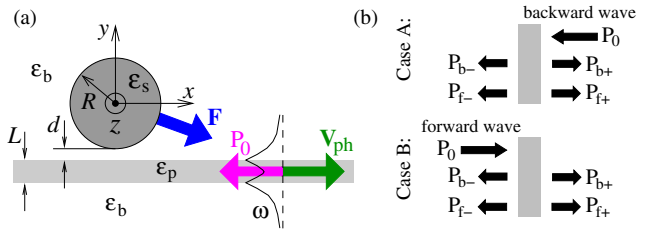

FIG. 1 (color online). (a) Realization of a pulling force: scattering of a guided backward wave creates a force on the particle that is opposite to the power flow of the initial wave. (b) Illustration of the two cases A and B studied.

Scattering creates guided waves that carry power from the particle. We label them according to Fig. 1(b), where the subscripts include the wave type (backward or forward) and the direction ($\pm x$) of the power flow. In addition to the guided waves, there is scattered bulk radiation with power P_s that goes to $y \to \pm\infty$. The guided modes with antisymmetric distribution of H_z are not excited since they are limited to $\omega/\omega_p < 1/\sqrt{2} \approx 0.71$.

We first calculate the electromagnetic fields and then find the force. We rely on the approach described in Ref. [11]. It is based on representing the fields outside of the particle as created by some effective surface current. The knowledge of the Green's function for the slab allows one to relate the currents to the fields near the particle. Matching the fields outside to that inside allows one to find the distribution of the effective current and the fields. The fields determine the force. Similar techniques are often used to solve diffraction problems [29–32].

To customize the approach of Ref. [11], which was applied to a plasma half-space, to the geometry of Fig. 1(a), we need to replace the reflection coefficient from the plasma half-space (Eq. (19) of Ref. [11]) with that from the plasma slab in the integral representation of the Green's function. The required reflection coefficient for a plane wave specified by the x component h of the wave vector is $r(h) = 2iABe^{i\phi_p}\sin\phi_p/(D_s D_a)$, with $D_{s,a} = B \mp Ae^{i\phi_p}$, $A = g_p/\varepsilon_p - g_b/\varepsilon_b$, $B = g_p/\varepsilon_p + g_b/\varepsilon_b$, $g_{p,b} = \sqrt{\varepsilon_{p,b}\omega^2/c^2 - h^2}$, $\phi_p = g_p L$. The poles of $D_{s,a}$ correspond to the symmetric and antisymmetric modes.

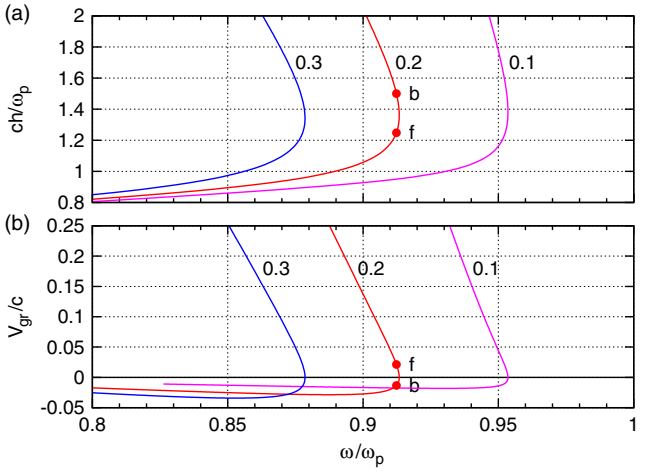

FIG. 2 (color online). Dispersion properties of mode (1) for $L\omega_p/c = 0.1$, 0.2, 0.3 (labeled next to the curves). (a) Wave number and (b) group velocity as functions of frequency. The dots show the operating points used in the simulations.

The numerical results were verified using two tests. The first test checked the balance of powers between the scattered waves (guided and bulk waves) and the initial wave. The second test checked the value of the force calculated using the Lorentz formula [see Eqs. (28) and (29) in Ref. [11]] and the difference in the momentum flows before and after scattering. In the studied range of kR ($k = \omega/c$), the relative error did not exceed 2×10^{-8} in the power balance and 2×10^{-7} in the momentum balance.

Let us now analyze case A, i.e., the scattering of the backward wave. The powers P_{b-}, P_{f+}, P_s and the force F_x as functions of kR for $kd = 1.2$ are shown in Fig. 3. An increase of kR results in a reduction of the transmitted backward wave. The transmission shows resonant features related to the excitation of WGMs. The scattered power is mostly split between the guided waves P_{b-}, P_{f+} and bulk waves P_s. The bulk radiation in the upper half-space exceeds that in the lower half-space. The powers P_{b+} and P_{f-} are not shown because their values do not exceed $10^{-3} \times P_0$. The creation of the forward wave propagating in the $+x$ direction corresponds to the reflection of the incident power and is consistent with the direction of wave circulation inside the resonator. The reflection is quite unusual since it does not occur in typical situations in which the suppression of transmission is accompanied by an increase in scattering only [11,32].

The force shown in Fig. 3(c) consists of a background and a set of large resonant peaks. The background level grows with kR and reaches $cF_x/P_0 \approx 0.2$ for $kR \gtrsim 10$. The peak positions correlate well with the transmission and scattering resonances. The magnitude of the peaks significantly exceeds (up to 4 times at $kR \approx 30$) the background level. It is remarkable that $F_x > 0$ in the whole range of $0 < kR < 30$. This means that the force is directed opposite to the power flow of the incident backward surface wave.

We now turn to case B, i.e., the scattering of the forward wave. The scattered powers and force are shown in Fig. 4 for the same $kd = 1.2$ as for Fig. 3. Increasing kR reduces the transmitted P_{f+} and gives rise to the reflected backward wave P_{b-}. The resonant dips in the reflection correlate with the peaks of the bulk radiation P_s. The force has a background (that can be negative) and large peaks. The peaks correspond to the propelling force in the direction of the incident power, in contrast to case A where the resonances give a pulling force.

To interpret the forces, we apply the concept of momentum flow to surface waves. The force produced within an arbitrary volume V is $\mathbf{F} = \int ds \boldsymbol{\mathcal{M}}$, where the momentum flow density (for real fields) is

$$4\pi \boldsymbol{\mathcal{M}}(\mathbf{n}) = \varepsilon(\mathbf{E}\cdot\mathbf{n})\mathbf{E} + \mu(\mathbf{H}\cdot\mathbf{n})\mathbf{H} - \frac{1}{2}(\varepsilon\mathbf{E}^2 + \mu\mathbf{H}^2)\mathbf{n},$$

where $\mathbf{n}$ is the normal to the surface surrounding V. We note that $\boldsymbol{\mathcal{M}}(\mathbf{n})$ is independent of the propagation direction. Assuming that a surface wave carries power in the $+x$ direction, the momentum flow that it creates entering V can be evaluated at the left boundary, see inset in Fig. 5:

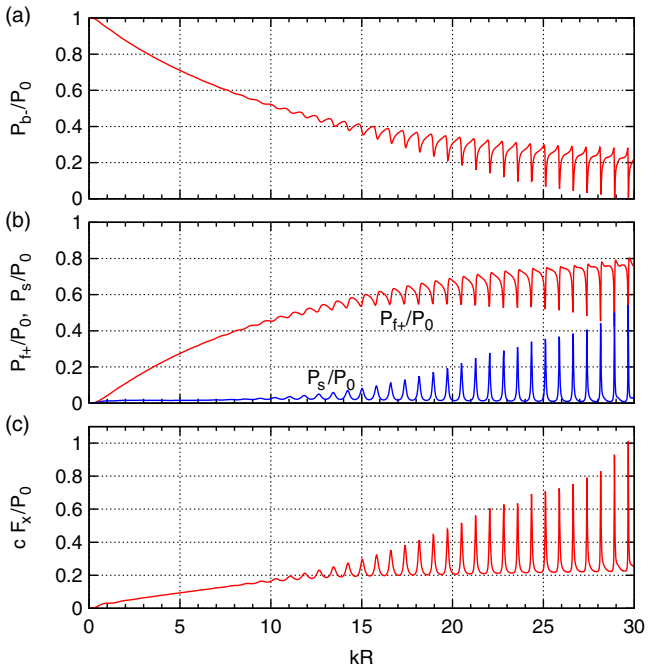

FIG. 3 (color online). Case A: Scattering of a backward wave. (a),(b) Powers of the modes and (c) force on the particle.

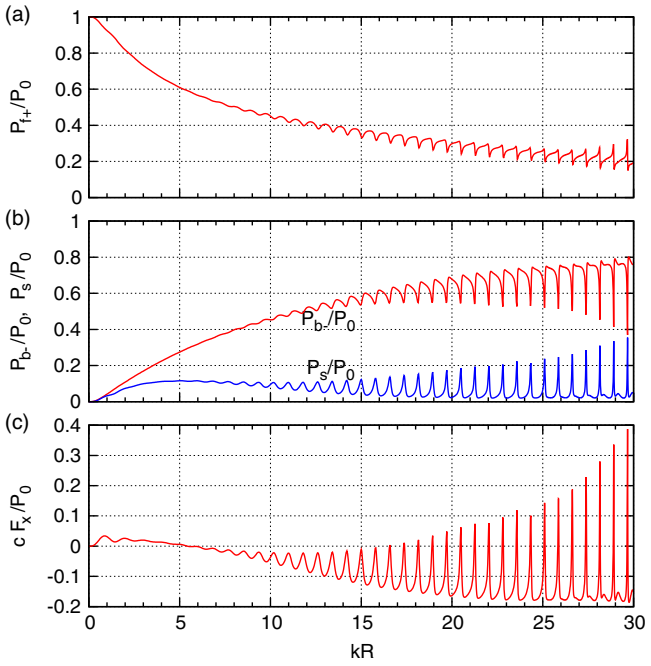

FIG. 4 (color online). Case B: Scattering of a forward wave. (a),(b) Powers of the modes and (c) force on the particle.

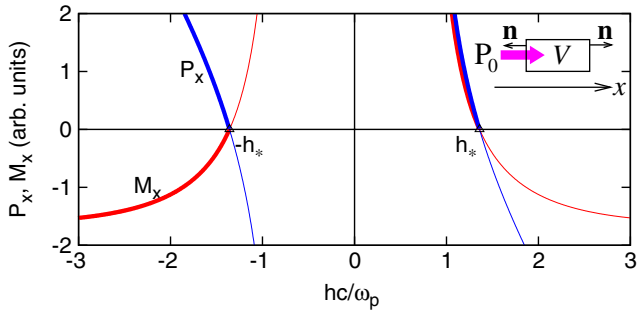

FIG. 5 (color online). Power P_x and momentum flow M_x for Eq. (1) as functions of h. The inset illustrates the wave entering an interaction region V. The thick lines correspond to $P_x > 0$.

$$M_x = \mathbf{x} \cdot \int ds \boldsymbol{\mathcal{M}}(-\mathbf{x}) = \frac{1}{4\pi} \int dy \varepsilon(|E_y|^2 - |E_x|^2) + |H_z|^2,$$

where $\mathbf{x}$ is the unit vector in the $+x$ direction. This expression for M_x holds both without [33] and with [34] material dispersion. The momentum flow M_x is equal to the force F_x it would create if the energy is absorbed.

Figure 5 shows the dependence of power P_x and momentum flow M_x on the wave number h for mode (1) at $L\omega_p/c = 0.2$ and a fixed H_0. The point $h = h_* > 0$ corresponds to the zero group velocity; see Fig. 2. The condition $P_x > 0$ holds on two intervals. The first interval ($h < h_*$) has $M_x > 0$ and corresponds to the forward wave. The second interval ($h < -h_*$) has $M_x < 0$ and corresponds to the backward wave. Thus, the entrance of the backward wave into V gives a negative momentum flow. We therefore can define the momentum flow for the surface wave that carries power P_0 in the $+x$ direction:

$$M_x = (h/\omega)P_0. \tag{2}$$

In Eq. (2), $h > 0$ corresponds to the forward wave while $h < 0$ corresponds to the backward wave. Although expression (2) was used before [33,34], its validity and consequences for backward waves were not discussed.

The force acting on the particle can be written as the difference between the momentum flow entering (input) M_x^e and leaving (output) M_x^o the interaction volume:

$$F_x = M_x^i - M_x^o, \tag{3}$$

where M_x^o includes the contributions from all excited guided and bulk waves. In case A, using Eq. (2) we obtain

$$M_x^i = \frac{h_b}{\omega} P_0 > 0, \tag{4a}$$

$$M_x^o = \frac{h_b}{\omega}(P_{b-} - P_{b+}) + \frac{h_f}{\omega}(P_{f+} - P_{f-}) + M_{sx}, \tag{4b}$$

where M_{sx} describes the momentum flow of bulk waves; see Eq. (36) in Ref. [11]. Note that $M_x^i > 0$ since the incident backward wave propagates in the $-x$ direction. We obtained that F_x calculated using the Lorentz formula agrees numerically with that using Eqs. (3) and (4). This means that the slab does not experience any x-directed force that may appear in some other situations [35]. Since M_{sx} is rather small (despite large P_s, see Ref. [11]), F_x can be estimated by using only P_{b-} and P_{f+}. The positive background force in Fig. 3(c) can be explained by a nonresonant reflection. The maximum force obtained is $cF_x/P_0 \approx 1$, which is comparable to the momentum flow of the incident backward wave $cM_x/P_0 = 1.644$. The difference is explained by the reflected P_{f+}. At WGM resonances, the reflected signal is actually reduced while bulk scattering and force are enhanced. The agreement between the force calculated using the Lorentz formula and that using the momentum difference was also checked for case B. The negative background in Fig. 4(c) can also be explained by the nonresonant power reflection into the backward wave and its large ($h_b > h_f$) wave number.

Let us briefly study the transverse force on the particle in cases A and B; see Fig. 6. The force remains negative (attractive) in the range $0 < kR < 30$ despite the presence of sharp peaks at resonances. The transverse force is not directly related to the incident momentum flow and may reach values higher than the longitudinal force. This may also be related to the particular choice of the waveguide. The attractive force may cause the particle to approach the waveguide and hit it. In practice, the pulling may not be a steady process but rather a series of events where the particle velocity changes rapidly. The changes can be recorded as in Ref. [10]. The pulling can also be observed by bringing the particle with optical tweezers to the waveguide and then releasing it.

To conclude, the force on a particle supporting WGMs excited by the surface waves of a plasma slab is investigated. It is shown that a backward wave can create a large resonant optical force directed opposite to the incident power. The pulling of the particle towards the energy source is shown to be consistent with the fact that the backward wave has its momentum flow opposite to the power flow. Although the negative momentum flow helps

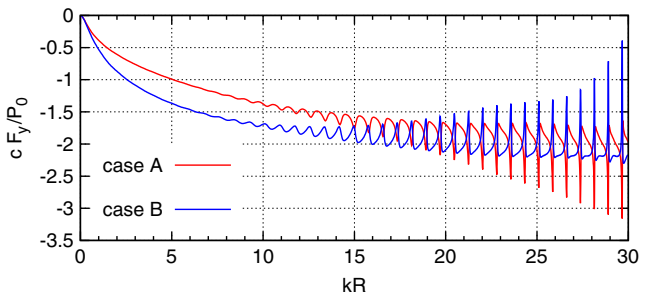

FIG. 6 (color online). Transverse force in cases A and B.

to create a pulling force, the actual value of the force depends on the distribution of the scattered power between all modes. Other backward-wave structures (for example, with periodic gratings [36] or dielectric filling [22,23]) are also expected to create the pulling effect. Similar to the dispersion in a plasma slab, a backward wave in structures with dielectric rods [22,23] is always accompanied by a forward wave with the same frequency but a different wave number.

The work was supported in part by the Ministry of Education and Science of the Russian Federation through Agreement No. 14.B37.21.0892. The author is grateful to Professor V. N. Astratov and Professor M. I. Bakunov for discussions.

*avmaslov@yandex.ru

[1] J. C. Maxwell, *A Treatise on Electricity and Magnetism* (Macmillan and Co., London, 1873), Vol. II, pp. 391.
[2] P. N. Lebedev, Ann. Phys. (Berlin) **311**, 433 (1901).
[3] A. Ashkin, *Proc. Natl. Acad. Sci. U. S. A.* **94**, 4853 (1997).
[4] W. N. Irvine, J. Opt. Soc. Am. **55**, 16 (1965).
[5] A. Ashkin and J. M. Dziedzic, Phys. Rev. Lett. **38**, 1351 (1977).
[6] V. Ilchenko and A. Matsko, IEEE J. Sel. Top. Quantum Electron. **12**, 15 (2006).
[7] H. Jaising, K. Grujić, and O. G. Helleso, Opt. Rev. **12**, 4 (2005).
[8] J. Ng and C. T. Chan, Appl. Phys. Lett. **92**, 251109 (2008).
[9] J. J. Xiao, J. Ng, Z. F. Lin, and C. T. Chan, Appl. Phys. Lett. **94**, 011102 (2009).
[10] Y. Li, O. V. Svitelskiy, A. V. Maslov, D. Carnegie, E. Rafailov, and V. N. Astratov, Light: Sci. Appl. **2**, e64 (2013).
[11] A. V. Maslov, V. N. Astratov, and M. I. Bakunov, Phys. Rev. A **87**, 053848 (2013).
[12] P. L. Marston, J. Acoust. Soc. Am. **120**, 3518 (2006).
[13] L. Zhang and P. L. Marston, Phys. Rev. E **84**, 035601(R) (2011).
[14] J. Chen, J. Ng, Z. Lin, and C. T. Chan, Nat. Photonics **5**, 531 (2011).
[15] S.-H. Lee, Y. Roichman, and D. G. Grier, Opt. Express **18**, 6988 (2010).
[16] A. Novitsky, C.-W. Qiu, and H. Wang, Phys. Rev. Lett. **107**, 203601 (2011).
[17] S. Sukhov and A. Dogariu, Phys. Rev. Lett. **107**, 203602 (2011).
[18] O. Brzobohatý, V. Karásek, M. Šiler, L. Chvátal, T. Čižmár, and P. Zemánek, Nat. Photonics **7**, 123 (2013).
[19] I. V. Krasnov, Phys. Lett. A **376**, 2743 (2012).
[20] T. Čižmár, V. Carcés-Chávez, K. Dholakia, and P. Zemánek, Appl. Phys. Lett. **86**, 174101 (2005).
[21] D. B. Ruffner and D. G. Grier, Phys. Rev. Lett. **109**, 163903 (2012).
[22] A. Salandrino and D. N. Christodoulides, Opt. Lett. **36**, 3103 (2011).
[23] P. J. B. Clarricoats and R. A. Waldron, J. Electron. Control **8**, 455 (1960).
[24] M. L Povinelli, M. Lončar, M. Ibanescu, E. J. Smythe, S. G. Johnson, F. Capasso, and J. D. Joannopoulos, Opt. Lett. **30**, 3042 (2005).
[25] M. Eichenfield, C. P. Michael, R. Perahia, and O. Painter, Nat. Photonics **1**, 416 (2007).
[26] P. T. Rakich, M. A. Popović, and Z. Wang, Opt. Express **17**, 18116 (2009).
[27] M. Li, W. H. P. Pernice, and H. X. Tang, Nat. Photonics **3**, 464 (2009).
[28] A. A. Oliner and T. Tamir, J. Appl. Phys. **33**, 231 (1962).
[29] V. I. Kalinichev and P. N. Vadov, Sov. J. Commun. Technol. Electron. **33**, 108 (1988).
[30] I. D. Chremmos and N. K. Uzunoglu, J. Opt. Soc. Am. A **21**, 839 (2004).
[31] A. G. Yarovoy, Microwave Opt. Technol. Lett. **7**, 178 (1994).
[32] S. V. Boriskina and A. I. Nosich, Microwave Opt. Technol. Lett. **13**, 169 (1996).
[33] J. Brown, *Proc. IEE* **113**, 27 (1966).
[34] H. A. Haus and H. Kogelnik, J. Opt. Soc. Am. **66**, 320 (1976).
[35] M. Mansuripur, Opt. Express **12**, 5375 (2004).
[36] V. N. Astratov, I. S. Culshaw, R. M. Stevenson, D. M. Whittaker, M. S. Skolnick, T. F. Krauss, and R. M. De La Rue, J. Lightwave Technol. **17**, 2050 (1999).